

Pentacene-carbon nanotubes: Semiconducting assemblies for thin-film transistor applications

X.-Z. Bo

DuPont, Central Research and Development, Wilmington, Delaware 19880 and Department of Chemistry and Columbia University Nanocenter, Columbia University, New York, New York 10027

N. G. Tassi

DuPont, Central Research and Development, Wilmington, Delaware 19880

C. Y. Lee and M. S. Strano

Department of Chemical and Biomolecular Engineering, University of Illinois at Urbana Champaign, Urbana, Illinois 61801

C. Nuckolls

Department of Chemistry and Columbia University Nanocenter, Columbia University, New York, New York 10027

Graciela B. Blanchet^{a)}

DuPont, Central Research and Development, Wilmington, Delaware 19880

(Received 6 January 2005; accepted 10 October 2005; published online 10 November 2005)

We demonstrate an alternative path for achieving high-transconductance organic transistors by assembling bilayers of pentacene onto random arrays of single-walled carbon nanotubes. We show here that, by varying the connectivity of the underlying nanotube network, the channel length of a thin-film transistor can be reduced by nearly two orders of magnitude—thus, enabling the increase of the device transconductance without reduction the on/off ratio. These field-induced percolating networks enable assembling high-transconductance transistors that, with relatively large source drain distances, can be manufactured with available commercial printing techniques. © 2005 American Institute of Physics. [DOI: 10.1063/1.2132063]

Organic thin-film transistors (TFTs) have been of great interest due to their potential applications in the fabrication of large-area, inexpensive devices for use in electrophoretic displays, storage and radio-frequency identification tags.^{1–3} Reaching such goals requires the fabrication of transistors with sufficiently large transconductance and on/off ratios. Since transconductance is proportional to the carrier mobility much of the effort has been focused on the development of novel organic semiconductors with higher carrier mobility.^{3,4}

However, transconductance also increases inversely with source to drain distance, thus providing a geometrical parameter to be modified for optimum device performance. In the semiconductor/carbon nanotube bilayer system described here, we explore such an approach: reduce the transistor channel length to increase transconductance.

Rather than improving mobility via new chemical structures, we exploited the formation of nearly percolating networks.^{4,5} By varying the connectivity of a random array of conducting rods joint by pentacene links evaporated on top, we achieved an effective reduction in channel length and thus an increase in the transconductance. The carriers take advantage of the conducting rods flowing partially within pentacene and partially through the rods. Thus, traveling only a fraction of the distance within the semiconductor leads to an effective channel length reduction.

Carbon nanotubes⁶ are used here as conducting rods for shortening the channel length. It has been previously demonstrated that random arrays of percolating single-walled car-

bon nanotubes (SWNTs) can form semiconducting^{7,8} and conducting^{9,10} percolating networks. While single tube carbon nanotube transistors have extremely high field-effect mobilities ($\sim 9000 \text{ cm}^2/\text{V s}$),⁸ random nanotube arrays have mobility of $\sim 10 \text{ cm}^2/\text{V s}$.^{9,10} In addition, they function in the percolating regime where metallic pathways across the transistor channel concurrently reduce the on/off switch function into unacceptable values.

In this letter we show that nearly percolating array of carbon nanotubes joint via semiconducting links can provide a significant advantage relative to random nanotube arrays enabling the increase of transconductance without significantly reducing the on/off ratio. In contrast, pentacene evaporated onto percolating SWNT networks shows, as random arrays,^{9,10} large effective mobilities with poor on/off ratio.

Hipco SWNT's ropes, fabricated by CNI, were separated into individual tubes^{9–12} with the aid of surfactants.^{13,14} The resulting aqueous dispersion containing metallic and semiconducting tubes was filtered and the surfactant fully removed. The tubes (and small diameter ropes) were dried and re-dispersed in ortho-dichloro benzene at 5, 10, 20, 35, and 50 mg/l concentrations. The various dispersions were spun at 1000 rpm onto a clean Si wafer with a 2500 Å thermal oxide and pre-patterned Au source/drain electrodes of various channel widths (W) and lengths (L). A 200 Å pentacene overlay evaporated at a base pressure of $\sim 7 \times 10^{-8}$ torr and at 0.2 Å/s, completed the device. Electrical performance was characterized using an Agilent 4155C.

Atomic force microscopy (AFM) images of SWNT arrays spun onto Si/SiO₂ wafers from 5 and 20 mg/l SWNT

^{a)} Author to whom correspondence should be addressed; electronic mail: graciela.b.blanchet@usa.dupont.com

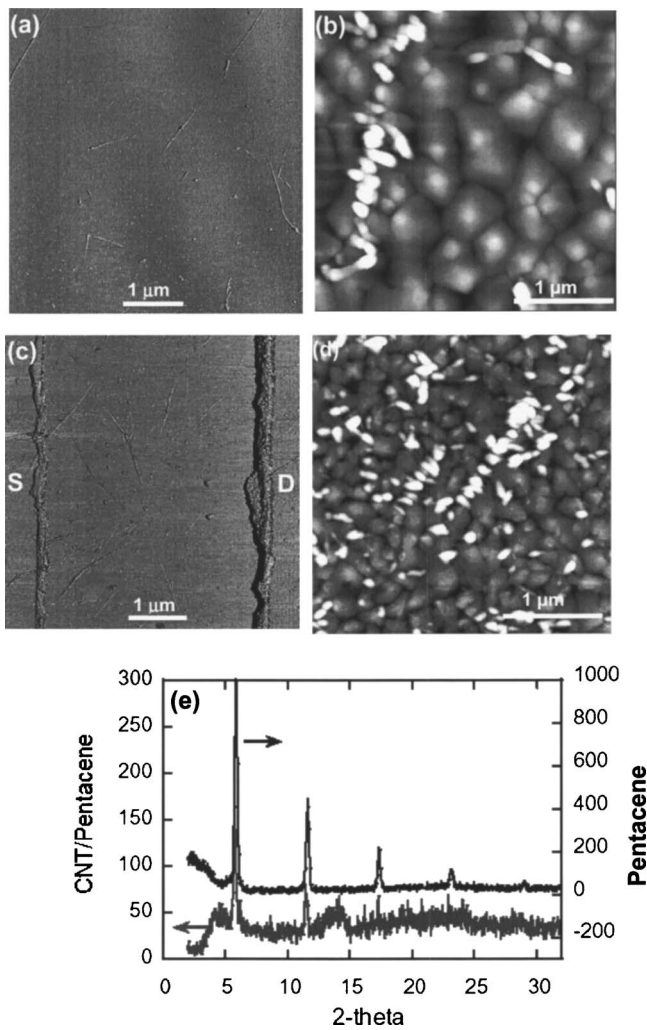
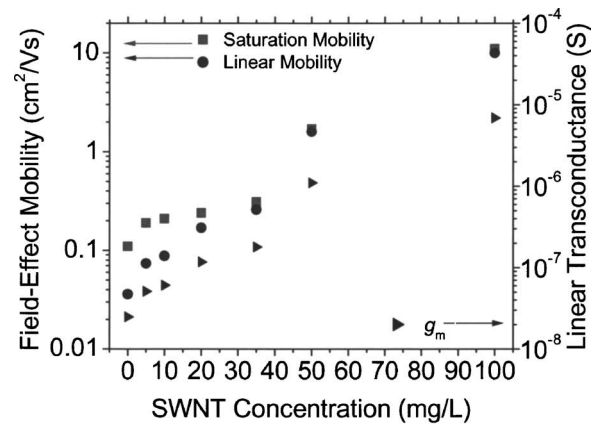


FIG. 1. AFM images of SWNTs spun from two different solution concentrations at (a) 5 mg/l and (c) 20 mg/l. (b) and (d) are AFM images of the corresponding bi-layers with 200-Å-thick pentacene evaporated at 0.2 A/s on top of SWNTs. The letter S and D indicate the Au source and drain electrodes. The x-ray diffraction spectra of 200 Å pentacene films evaporated at 0.2 A/s onto bare SiO_2 and onto a SWNT array spun onto SiO_2 dispersion are shown in (e).

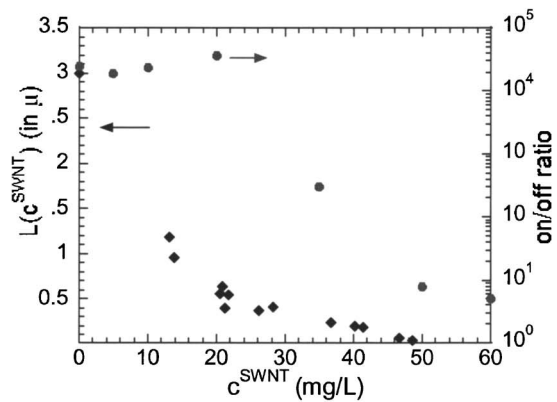
dispersions and the corresponding SWNT/pentacene bilayers are shown in Figs. 1(a)–1(d). The structure of the pentacene bilayers was determined by x-ray diffraction (XRD) in a symmetric reflection, coupled θ – 2θ mode at a $\lambda'_{\text{K}\alpha 1}$ wavelength of 1.5406 Å. The x-ray diffraction spectra of pentacene evaporated onto SiO_2 and of pentacene evaporated onto an array of SWNT spun on SiO_2 from a 20 mg/l solution are shown in Fig. 1(e).

The effective linear and saturation mobilities¹³ and transconductance of pentacene-SWNT TFTs bilayers as a function of SWNT concentrations are shown in Fig. 2(a). Both parameters increase by about $5\times$ from 0.036 to 0.17 $\text{cm}^2/\text{V s}$ and $2.48 \cdot 10^{-8}$ – $1.17 \cdot 10^{-7}$ S as the underlying SWNT network approaches percolation.

Figure 2(b) shows the channel length $L(c)$ for random arrays for tubes and on/off ratio for bilayer devices as a function of SWNT content. The channel length of the random array of tubes decreases exponentially with increasing SWNT concentration reaching percolation at 50 mg/l, the onset of the rapid reduction in on/off ratio. Although the effective mobility and transconductance reach $10 \text{ cm}^2/\text{V s}$ at high carbon nanotube concentration, a concurrent increase in



(a)



(b)

FIG. 2. (a) Effective linear and saturation mobilities of TFT pentacene bilayers as a function of the SWNT concentrations. Mobilities are calculated from TFT transfer characteristics at $V_{\text{ds}} = -50$ V in the saturation region (circles) and at $V_{\text{ds}} = -5$ V in the linear region (squares). Linear transconductance corresponds to $V_{\text{ds}} = -5$ V, labeled by triangles. (b) The channel length of nonpercolating arrays of SWNT as a function of increasing SWNT content and on/off ratio of bottom gate devices (at $V_{\text{ds}} = -50$ V) for various SWNT concentrations are shown in diamonds and circles, respectively in (b).

off current leads to on/off^{8,9} ratios of less than 10 as the SWNT concentration approaches 100 mg/l.

Although the system described here is a bilayer of conducting rods of varying connectivity with a semiconducting overlay, some aspects are similar to those expected from conducting rods directly dispersed in an insulating matrix. Both exhibit a percolation threshold that represents the onset to the formation of conducting path. In TFT devices comprising nonpercolating networks the presence of conducting SWNT rods merely reduces the distance between source and drain. In contrast, conducting pathways above percolation lead to a rapid increase in off current, thus lowering of the on/off ratio.

We have recently shown that the mobility of a soluble semiconductor, polythiophene (PTH), can be increased up to $60\times$ by the addition of a nonpercolating SWNT network.⁵ Since the mobility of the PTH host remained unchanged, the increase in transconductance was solely attributed to a reduction of the channel length. Although these composites have the great advantage of being casted from solution, soluble semiconductors have low mobilities. Thus, the increase in transconductance is insufficient for many electronic applications. In contrast, bilayers have the promise of higher mo-

bilities. The underlay of tubes offers a similar channel length reduction while semiconducting overlays of much higher mobility semiconductor can be explored. In that vein, we chose pentacene as the overlay to be evaporated onto a non-percolating SWNT array.

As in the single layer composite work, the majority of the current paths between source and drain follow the highly conducting nanotubes with short, switchable pentacene links completing the circuit. In principle, one would expect the increase in transconductance to scale, inversely with channel length reduction,¹⁴ and that the channel length reduction be essentially the same order of magnitude as in Ref. 5. Thus, a nearly two orders of magnitude increase in transconductance reflecting a 100× reduction in channel length. Figure 2 shows that the channel length of the SWNT underlay indeed decreases by two orders of magnitude as the network approaches percolation. However, the transconductance of the pentacene bilayer increases merely by a factor of 5×. Since transconductance is proportional to mobility and inversely proportional to channel length, the results in Fig. 2 suggest that the 100× decrease in channel length is accompanied by a 20× decrease in the mobility of the pentacene overlay.

The effective channel length in Fig. 2(b) was estimated from AFM images of nonpercolating nanotube arrays spun at 1000 rpm onto the pre-patterned wafers from 5, 10, 20, 35, and 50 mg/l SWNT dispersions. By using pattern recognition tools, nanotubes were identified and pathways selected. The channel lengths were obtained by adding the various breaks along each possible path. The total number of tubes/ μ^2 measured for each image. The channel length $L(c)$ for each concentration, c , was the average of the many path lengths obtained for several images at each of the concentrations. Although this is a very tedious and somewhat subjective procedure consistent, reproducible results were obtained. The data were fitted to $L(c) = 3.05 \exp(-0.078c)$.

The x-ray data in Fig. 1 show that as the concentration of the SWNT increases, the intensity of the crystalline peaks is severely reduced.

Dimitrakopoulos¹⁴ nicely illustrated the relationship between XRD spectra and mobility for pentacene—amorphous where practically insulating ($\mu \sim 10^{-8}$ cm²/V S) while very ordered crystalline film are grown at ambient temperature ($\mu \sim 10^{-1}$ cm²/V S). As shown in Fig. 1(e), the pentacene control shows four peaks that can be indexed (001) reflections at 2θ 5.74, 11.45, 17.26 and 23.15 and grain size of ~ 2 μ m. The d_{001} value corresponds to a spacing of 15.4 Å in agreement to what was previously reported for thin-film phase structures.¹⁴ In contrast, the 20 mg/l spectra shows a decrease in the intensity of the crystalline peaks is accompanied by large increase in the amorphous background. In addition, the AFM shows that pentacene evaporated onto tubes spun from 20 mg/l dispersion has smaller grains (~ 0.1 μ m). Since a 10–20× decrease in grain size increase the number of grain boundaries between source and drain with a decrease in mobility.¹⁵ The rapid decrease of intensity and absence of the higher order peaks for the 20 mg/l spectra further suggest a significantly larger static Debye Waller

factor with a higher degree of short range disorder along the c^* axis.

Finally, the electrical properties of percolating bilayers are similar to that of percolating random arrays of carbon nanotubes. The effect of the pentacene overlay is minimal, perhaps modifying the tube-to-tube contact resistance and reducing hysteresis by passivating the nanotube surface.¹⁶ As for random SWNT arrays, percolating bilayers exhibit high mobilities and poor on/off ratios.

In conclusion, we have created a short channel length transistor through the exploitation of nonpercolating SWNT arrays that are connected via pentacene links. This method can potentially raise the transconductance of our device by two orders of magnitude. The factor of 5 observed here for pentacene bilayers reflects a significant lowering of the pentacene crystallinity and not the inherent advantage of this approach. The full potential of the bilayers can perhaps be achieved with amorphous semiconductor that with compatible morphologies conform to the underlying network of tubes. Since the origin of this mobility improvement relies on the reduction of the effective source drain distance via the formation of a nonpercolating arrays of SWNTs, on/off ratio of 10^5 can be maintained. In contrast, mobilities of 50 cm²/V s can be achieved for bilayers with percolating SWNT networks although the on/off ratios are then reduced by 3–4 orders of magnitude.

The authors thank the Nanoscale Science and Engineering Initiative of the National Science Foundation under Award No. CHE-0117752, the New York State Office of Science, Technology, and Academic Research (NYSTAR), and NSF SGER Award No. ECS-04-08059 for support.

¹H. Sirringhaus, N. Tessler, and R. H. Friend, *Science* **280**, 1741 (1998).

²G. B. Blanchet, Y. L. Loo, J. A. Rogers, C. R. Fincher, and F. Gao, *Appl. Phys. Lett.* **82**, 463 (2003).

³C. D. Dimitrakopoulos and P. R. L. Malenfant, *Adv. Mater. (Weinheim, Ger.)* **14**, 99 (2002).

⁴G. B. Blanchet, S. Subramoney, and C. Nuckolls, *Appl. Phys. Lett.* **85**, 828 (2004).

⁵X. Z. Bo, M. Strano, C. Nuckolls, and Graciela Blanchet, *Appl. Phys. Lett.* **86**, 182102 (2005).

⁶M. Shtein, J. Mapel, J. B. Benziger, and S. R. Forrest, *Appl. Phys. Lett.* **81**, 268 (2002).

⁷L. Torsi, A. Dodabalapur, and H. E. Katz, *J. Appl. Phys.* **78**, 1088 (1995).

⁸M. S. Fuhrer, B. M. Kim, T. Durkop, and T. Brintlinger, *Nano Lett.* **2**, 755 (2002).

⁹E. S. Snow, J. P. Novak, P. M. Campbell, and D. Park, *Appl. Phys. Lett.* **82**, 145 (2003).

¹⁰M. S. Strano, C. A. Dyke, M. L. Usrey, P. W. Barone, M. J. Allen, H. W. Shan, C. Kittrell, R. H. Hauge, J. M. Tour, and R. E. Smalley, *Science* **301**, 1519 (2003).

¹¹M. S. Strano, V. C. Moore, M. K. Miller, M. J. Allen, E. H. Haroz, C. Kittrell, R. H. Hauge, and R. E. Smalley, *J. Nanosci. Nanotechnol.* **3**, 81 (2003).

¹²M. S. Strano, *J. Am. Chem. Soc.* **125**, 16148 (2003).

¹³S. M. Sze, *Semiconductor Devices, Physics and Technology* (Wiley, New York, 1985).

¹⁴C. D. Dimitrakopoulos, A. R. Brown, and A. Pomp, *J. Appl. Phys.* **80**, 2501 (1996).

¹⁵M. Shtein, J. Mapel, J. B. Benziger, and S. Forrest, *Appl. Phys. Lett.* **81**, 268 (2002).

¹⁶W. Kim, A. Javey, O. Vermesh, Q. Wang, Y. Li, and H. Dai, *Nano Lett.* **3**, 193 (2003).